

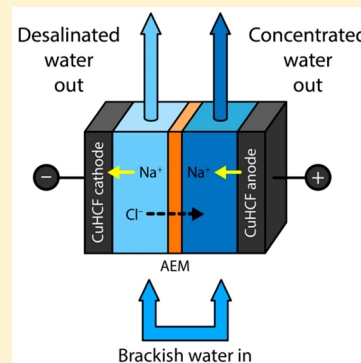
Low Energy Desalination Using Battery Electrode Deionization

Taeyoung Kim, Christopher A. Gorski,^{1b} and Bruce E. Logan^{*1b}

Department of Civil and Environmental Engineering, The Pennsylvania State University, University Park, Pennsylvania 16802, United States

S Supporting Information

ABSTRACT: New electrochemical technologies that use capacitive or battery electrodes are being developed to minimize energy requirements for desalinating brackish waters. When a pair of electrodes is charged in capacitive deionization (CDI) systems, cations bind to the cathode and anions bind to the anode, but high applied voltages (>1.2 V) result in parasitic reactions and irreversible electrode oxidation. In the battery electrode deionization (BDI) system developed here, two identical copper hexacyanoferrate (CuHCF) battery electrodes were used that release and bind cations, with anion separation occurring via an anion exchange membrane. The system used an applied voltage of 0.6 V, which avoided parasitic reactions, achieved high electrode desalination capacities (up to 100 mg-NaCl/g-electrode, 50 mM NaCl influent), and consumed less energy than CDI. Simultaneous production of desalinated and concentrated solutions in two channels avoided a two-cycle approach needed for CDI. Stacking additional membranes between CuHCF electrodes (up to three anion and two cation exchange membranes) reduced energy consumption to only 0.02 kWh/m³ (approximately an order of magnitude lower than values reported for CDI), for an influent desalination similar to CDI (25 mM decreased to 17 mM). These results show that BDI could be effective as a very low energy method for brackish water desalination.



INTRODUCTION

Conventional desalination technologies can produce freshwater from seawater and brackish water using heat (e.g., thermal distillation) or an applied pressure (e.g., membrane-based reverse osmosis),¹ but each faces challenges. Thermal distillation processes are simple and effective for seawater desalination, but they require high amounts of energy per volume of freshwater produced (5–60 kWh/m³).^{2,3} Reverse osmosis forces water molecules through a semipermeable membrane¹ and has lower energy demands that range from 0.5–2.5 kWh/m³ for brackish water (<10 g/L) to 3–4 kWh/m³ for seawater (~ 35 g/L).^{4–6} The main challenge with reverse osmosis is that the flow of water through semipermeable membranes leads to rapid fouling, which decreases performance due to the need for frequent membrane cleaning.^{7,8}

Electrochemical techniques offer an alternative means to desalinate water. Several electrochemical approaches have been proposed, including electrodialysis (ED),⁹ capacitive deionization (CDI),¹⁰ shock electrodialysis,¹¹ and ion concentration polarization.¹² Among these, ED is the most common, where desalination occurs within a large stack of alternating cation and anion exchange membranes. In ED, ion transport into the electrode channels is achieved either by sacrificial reactions (such as water splitting and hydrogen gas production) or facilitated using soluble redox couples (e.g., hexacyanoferrate), and thus, the electrodes in ED are not used for desalination. CDI is a relatively newer desalination approach based on ion separation using electrodes, rather than in a stack of membranes as in ED. A typical CDI cell consists of two capacitive (i.e., nonfaradaic) electrodes, such as activated

carbon, that remove salt ions via electrostatic interactions when a current is applied to the cell in the first cycle and release salt ions in a second cycle (release of brine) by alternating the direction of the applied current. The use of inexpensive electrodes, no membranes, and low energy requirements (<0.5 kWh/m³ for <2 g/L)⁵ could make CDI more competitive than RO or ED for desalination of brackish water. CDI systems have been modified to improve performance by covering electrodes with IEMs or ion exchange polymers (MCDI).^{13–15} Energy recovery in the second cycle has been proposed to reduce energy requirements,^{16,17} although this is technically challenging due to the high internal resistance. Two-cycle operation of the feedwater can be avoided by using flow electrodes, although this increases energy requirements for pumping.^{18–23} Practical applications of CDI systems have been limited by low salt adsorption capacities at an applied voltage of 1.2 V and parasitic reactions. CDI performance can be improved by using a larger voltage window, but this accelerates parasitic reactions that damage electrodes and reduce energy efficiency through carbon electrode oxidation, H₂O₂ generation, and hydrogen gas production.^{10,22,24–31}

Battery (i.e., faradaic) electrodes can provide higher capacities for desalination than capacitive electrodes due their abilities to store salt ions within their crystal structures,^{32–36} and they can theoretically reduce energy consumption and

Received: September 3, 2017

Revised: September 15, 2017

Accepted: September 18, 2017

Published: September 21, 2017

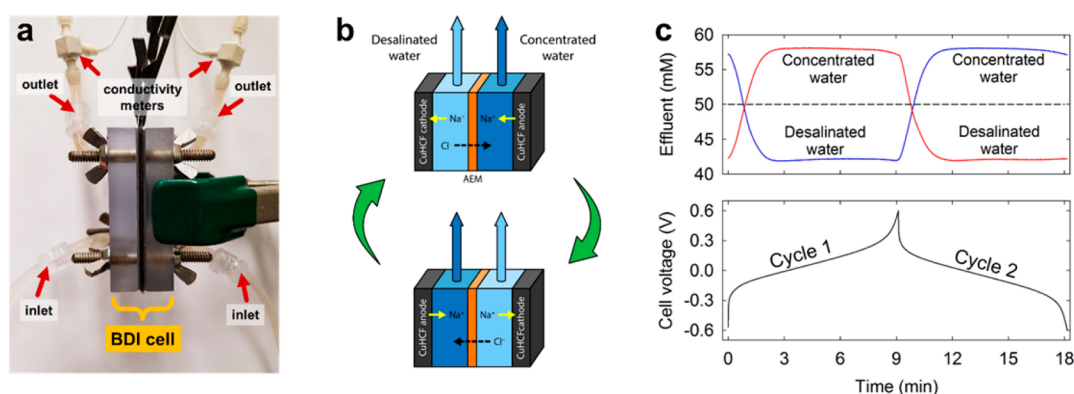


Figure 1. (a) Photo of experimental setup, showing a side view of BDI cell, inlet/outlet tubing, and conductivity meters. (b) Schematic diagram of single-stacked BDI cell with directions of Na⁺ and Cl⁻ in each cycle. Release/uptake of Na⁺ by copper hexacyanoferrate (CuHCF) electrodes (solid arrows) drove the transport of ions through the AEM (dashed arrows), allowing for desalination and concentration. (c) Representative effluent concentration and cell voltage profiles in a single-stacked BDI cell (influent: 50 mM NaCl; flow rate: 0.5 mL/min; current density: ± 7 mA or 9.9 A/m²).

avoid parasitic reactions through the use of a smaller voltage window. Numerous battery electrode materials that interact with Na⁺, including sodium manganese oxide, sodium iron pyrophosphate, and Prussian blue analogues,^{32–37} have yielded higher desalination capacities than CDI. In contrast, there is a lack of battery electrodes that interact with Cl⁻. Ag has been used for Cl⁻ removal,^{32,35} which is not practical due to its high cost. Recently, the use of two channels separated by a membrane was shown to desalinate water as well as produce electricity from salinity gradients without the need for an electrode that interacts with Cl⁻,^{37–42} suggesting that a two-channel system could be a viable means for desalination that overcomes the intermittent desalination and the need for an asymmetric electrode pair.

Here, we developed an improved approach for water desalination that increases desalination capacity compared to CDI by using two identical battery electrodes that interact only with Na⁺, with the channels separated by at least one anion exchange membrane, referred to as battery electrode deionization (BDI). The use of two identical battery electrodes (copper hexacyanoferrate, CuHCF) in separated channels, versus two different battery electrodes in a single channel,^{32,35,43} enabled simultaneous and continuous production of desalinated and concentrated solutions. Adding additional membranes improved performance based on both accomplishing ion removal with the electrodes (similar to CDI) and with the membranes (similar to ED). The feasibility of this approach was investigated using BDIs with single and multiple membranes and by testing the system with different influent salt concentrations to achieve salt removals similar to those previously evaluated for CDI and MCDI systems (typically less than 100 mM influent).^{44,45}

MATERIALS AND METHODS

Electrode Preparation. CuHCF was prepared by a coprecipitation method as previously reported.^{39,46} Briefly, 100 mL of 0.1 M Cu(NO₃)₂ (Sigma-Aldrich) and 100 mL of 0.05 M K₃[Fe(CN)₆] (J.T.Baker) were added dropwise to 50 mL of deionized water under vigorous stirring at room temperature. Resulting precipitates were washed and collected using a centrifuge, followed by overnight drying in a vacuum oven at 70 °C. CuHCF electrodes were prepared by mixing CuHCF powder (86 wt %), carbon black (7 wt %, Vulcan

XC72R, Cabot), and polyvinylidene fluoride (7 wt %, kynar HSV 900, Arkema Inc.) in 1-methyl-2-pyrrolidinone (Sigma-Aldrich). The mixture was loaded onto carbon cloth (1071HCB, AvCarb Material Solutions) by drop-casting using a pipet, and then, the solvent was removed by drying at 70 °C. Before performing desalination experiments, 0.35 V was applied to one CuHCF electrode (Na⁺ intercalation) and 1 V was applied to the other CuHCF electrode (Na⁺ deintercalation) in a 3-electrode electrochemical cell with an Ag/AgCl reference electrode (3 M NaCl).

Cell Construction. Desalination experiments were performed in a custom-built flow cell (Figure 1a). Gaskets provided circular water flow channels (area = 7.07 cm²) with a fabric spacer (Sefar Nitex 03–160/53, thickness = 100 μm). Each channel was separated by an anion exchange (AEM, Selemon AMV, Asahi Glass, Japan) or cation exchange membrane (CEM, Selemon CMV), and CuHCF electrodes were placed at each end of the channel with graphite foil as a current collector. The single-stacked cell consisted of two channels separated by an AEM, and the number of channels doubled (i.e., double-stacked cell) or tripled (i.e., triple-stacked cell) by adding an alternative arrays of AEMs and CEMs (Figure S1).

Desalination Experiments. To evaluate desalination performance, each channel was fed by a 50 mM NaCl solution (except as noted) at a flow rate of 0.5 mL/min while applying constant current to the cell using a potentiostat (VMP3, Bio-Logic). Several current densities between 1 and 10 mA (1.4 and 14.1 A/m²) were used in the cell voltage range between -0.6 to +0.6 V, depending on the number of stacks. The current was reversed when the cell voltage reached -0.6 V or +0.6 V. Cyclic operation produced desalinated and concentrated solutions at the alternating outlets for each cycle (Figure 1b). The effluent conductivity was recorded using two flow-through conductivity meter electrodes (ET908, eDAQ, Australia) located at each cell outlet. The effluents were not recycled.

Data Analysis. Conductivity data were converted to concentrations by assuming that the concentration was linearly proportional to the conductivity. The amount of ions (i.e., Na⁺ and Cl⁻) separated was calculated by integrating the difference between influent and effluent concentrations over the course of charge and discharge and multiplying it by the flow rate. Dividing the mass of ions separated by the total mass of both

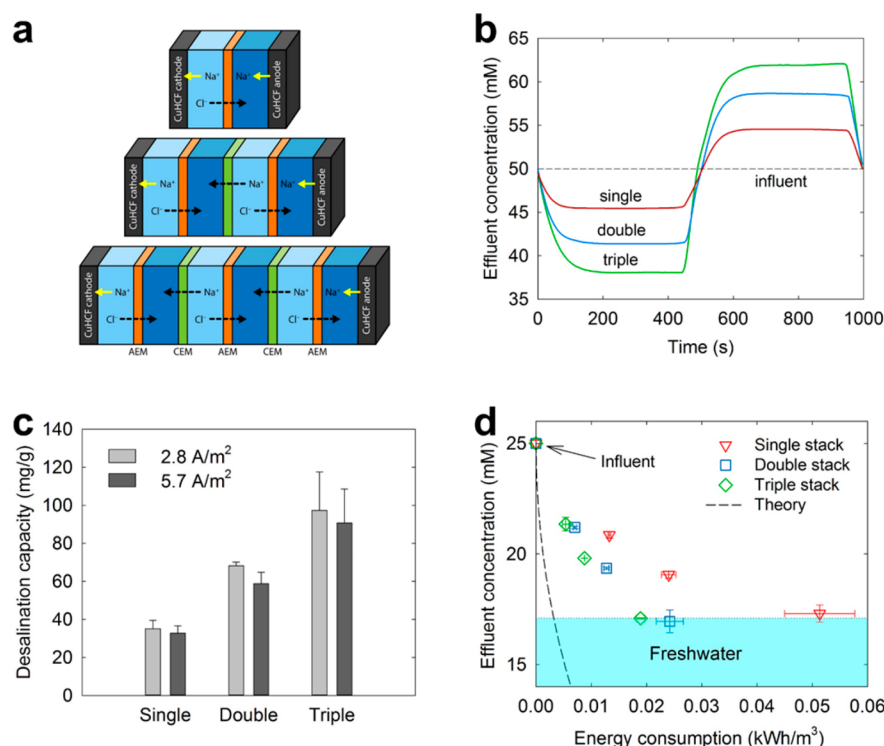
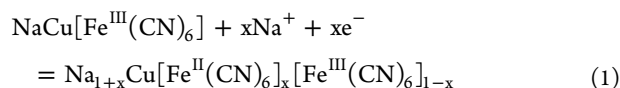


Figure 2. (a) Schematic describing a BDI cell how AEMs and CEMs were stacked between CuHCF cathode and anode. (b) The effect of stacking IEMs on the effluent concentration at a fixed flow rate of 0.5 mL/min and current density of 5.7 A/m² (influent: 50 mM NaCl). Duration of a cycle was 500 s. (c) Initial desalination capacity as functions of the number of stacks and current density in 50 mM NaCl. Error bars show the range based on triplicate experiments. (d) Effluent concentration as a function of energy consumption for different numbers of IEM stacks in the BDI (influent: 25 mM NaCl). The use of a higher current density produced a lower effluent concentration; thus, more energy was consumed based on the volume of desalinated water (50% water recovery). Increasing the number of stacks reduced energy consumption, which approached closer to the theoretical minimum (dashed line). Error bars show the range based on duplicate experiments.

electrodes yielded the desalination capacity in a single cell (mg_{NaCl}/g_{electrode}), analogous to “salt adsorption capacity”. We did not use that term here because salt was removed/released via redox reactions involving electrodes and ion transport through IEMs and not by adsorption. Average values of the desalination capacities (triplicate experiments) were derived from both effluents and their desalinated and concentrated solutions. The energy consumed in an experiment was normalized to the amount of desalinated water (kWh/m³, Figure S2), where the volume of desalinated and concentrated solutions were the same (i.e., 50% water recovery).

RESULTS AND DISCUSSION

Desalination Performance. To demonstrate the feasibility of the BDI, we examined the desalination performance of a BDI cell containing two identical CuHCF electrodes and an AEM fed with synthetic brackish water (50 mM NaCl; 2.9 g/L). When a constant current of 7 mA (9.9 A/m²) was applied to the cell, the influent water was desalinated by 14% (to 43 mM) (Figure 1c). During the desalination process, the CuHCF cathode was reduced with Na⁺ uptake from the solution in catholyte channel, and the CuHCF anode was oxidized with Na⁺ release to the solution in anolyte channel according to the following half reaction:^{39,42,46}



CuHCF can also interact with other cations, including Li⁺, K⁺, NH₄⁺, Ca²⁺, and Mg²⁺,^{47,48} and therefore, other cations in water would also be removed in this system. Reactions occurring at CuHCF electrodes resulted in Cl[−] ion transport from catholyte to anolyte channels through the AEM. Thus, desalinated solution was produced in a catholyte channel, and concentrated solution was produced in anolyte channel. Over the course of charging or discharging, the cell voltage gradually changed between −0.3 and 0.3 V, and then sharply approached the voltage limit (±0.6 V). The sharp increase or decrease in the cell voltage indicated that the capacity of each CuHCF electrode was fully utilized near this voltage limit, so that no additional Na⁺ uptake or release could have occurred (Figure S3).

Effect of Adding an Alternative Array of IEMs. To increase the extent of desalination using the voltage range as before (±0.6 V) while maintaining the current, we added different numbers of IEMs between the electrodes to form a hybrid system based on both electrode and membrane ion separation (Figure 2a). At a fixed flow rate of 0.5 mL/min and constant current of 4 mA (5.7 A/m²), the concentration difference between influent and effluent increased from ~4 mM in a single-stacked cell to ~8 mM in a double-stacked cell and ~12 mM in a triple-stacked cell (Figure 2b). The different effluent concentrations resulted from the retention time per channel for the same current transferred between the electrodes. If the same flow rate per channel is used, the same effluent concentration with a larger volume could be produced as the number of stacks is increased, as long as the

cell voltage is sufficient to drive current with the increased resistances of more membranes and cells.

The increase in ion separation by adding a small stack of IEMs also magnified desalination capacity based on the mass of two CuHCF electrodes in a single cell. The initial desalination capacity achieved in the triple-stacked cell with 50 mM NaCl was nearly 100 mg/g at the lowest current density of 2.8 A/m² (Figure 2c), which was the highest value reported using capacitive or battery electrodes. Applying a higher current density produced a lower effluent concentration (Figure S4), but it resulted a decrease in desalination capacity. Increasing the desalination capacity would be possible by improving charge utilization of CuHCF electrodes because the charge utilization in the current system was only ~60% of the full capacity of CuHCF electrodes, which was 89 C/g in a full cell (based on a half-cell measurement in 1 M NaCl, Figure S5), equivalent to 162 mg/g in a triple-stacked BDI cell. Among the full capacity, only ~70 C/g was applied to the BDI cell at a low current density (2 mA or 2.8 A/m²) due in part to the decreased salt concentration (0.05 M NaCl, Figure S5) and increased cell resistance. Additional loss occurred when the charge was used for separating ions, resulting in a charge efficiency of ~80%.

Energy Consumption. To examine the amount of energy consumed relative to a previous study, which reported desalination of brackish water to freshwater levels in MCDI,⁵ we used an influent salt concentration of 25 mM (1.5 g/L) and desalinated the water to that of freshwater (17 mM, 1 g/L). The energy consumption per volume of water treated was significantly reduced as the number of IEMs was increased from a one (single-stacked cell) to five (triple-stacked cell) (Figure 2d). The energy consumption of the triple-stacked cell of 0.02 kWh/m³ (0.01 kWh/kg-NaCl) was nearly 10 times lower than the energy reported for CDI with IEMs for the same influent and effluent concentrations (~0.2 kWh/m³).⁵ Energy recovery in BDI is theoretically possible based on capturing energy at the beginning of the cycle when the flows are switched, similar to that proposed for the second cycle in CDI,^{5,17} but it does not seem to be worthwhile for the current BDI system (Figure S6).

Desalination of a higher influent salt concentration (>25 mM) to that of freshwater (17 mM, 1 g/L) could be achieved by technological advancements, especially by using a larger BDI cell because the net applicable current is limited by the area. To demonstrate how a BDI cell could increase the extent of desalination, we connected two double-stacked BDI cells in series, providing more surface area for desalination. This enabled desalination of 34 mM (2 g/L) to 17 mM (1 g/L) with energy consumption of 0.07 kWh/m³ (0.07 kWh/kg-salt, Figure S7). In addition, desalination of 50 mM (2.9 g/L) below 17 mM (1 g/L) was achieved by recycling a small volume of (~1 mL) solutions, which consumed 0.16 kWh/m³ (0.34 kWh/kg). The energy consumption in these experiments was less than previous results using MCDI (Figure S8),⁵ supporting that low energy desalination would be possible using BDI over a wider concentration range. Further investigations are needed to determine the net energy consumption when scaled up, which may require additional energy input to operate the system.

The energy reduction can be evaluated based on the factor of $1/n$, where n is the number of stacks (e.g., $n = 2$ for the double-stacked cell with 1 CEM and 2 AEMs), as the current needed to achieve a freshwater effluent concentration was $1/n$ of the current used for a single-stacked cell. Although stacking additional IEMs could further reduce the energy consumption approaching closer to the theoretical minimum (~0.003 kWh/

m³, dashed line in Figure 2d, also see Supporting Information), other factors must be considered such as the cost of the additional IEMs relative to performance due to increased cell resistance. For example, the use of a triple-stacked cell reduced the energy consumption by 1/3, but it required 5 times more IEMs than a single-stacked cell. The use of more IEMs also increased ohmic resistances due to the additional membranes and flow channels, resulting in a decrease in the highest applicable current density (Figure S4).

Outlook. The use of battery electrodes combined with a small number of IEMs in a BDI cell achieved a 10-fold reduction in the energy consumption compared to the lowest value reported to date for brackish water desalination under similar feed and product conditions. The cell voltage (0.6 V) was lower than that used in a CDI system (1.2 V), and the cell architecture enabled continuous operation as opposed to the two-cycle, single-channel cell CDI and desalination battery systems. The battery electrodes had a high capacity for salt and did not suffer from parasitic reactions within the voltage window used here. There are challenges that remain for further development of this BDI system. For example, a 50-cycle test using the CuHCF electrodes resulted in a 30% decrease in applied charge to the cell (Figure S9a), which suggested the occurrence of an irreversible electrode reaction. This deterioration was unexpected because CuHCF electrodes have shown good cycling performance in battery applications (83% retention after 40,000 cycles in 1 M KNO₃).⁴⁶ However, reduced performance was obtained with a sodium-based electrolyte (77% retention after 500 cycles).⁴⁸ Since Prussian blue analogues are less susceptible to dissolution only under mild acidic conditions,⁴⁹ it was possible that the CuHCF electrodes could have dissolved at pH 7 used here. However, a 50-cycle test at pH 4 and 20-cycle test at pH 2 showed a similar reduction in performance, and therefore, the pH was not a factor (Figure S9a). One solution to improve the cycle stability was adjusting the voltage range from ± 0.6 to ± 0.3 V, as this produced only a 14% reduction after 50 cycles (Figure S9b, S9c, S9d). One explanation for the decrease would be that the dissolution of CuHCF occurred by applying potential to the electrode, which is supported by the constant charge efficiency over the cycles (~80%) and yellow stain observed on AEM after the cycling test. Although low concentrations of copper (<1.3 mg/L, drinking water standard) and ferricyanide (an approved food additive) ions in drinking water are safe for human consumption,⁵⁰ the decrease in performance due to damage or loss of electrode materials clearly warrants further investigation.

The most economical BDI configuration will depend on the cost of the materials, particularly the IEMs. Based on the results obtained here, using a double-stacked cell (1 CEM and 2 AEMs) provided a good balance between desalination performance and the need to minimize the number of IEMs due to their high cost. The main advantage of the BDI compared to MCDI or ED is that desalination occurs in both the electrode and membrane channels. CDI has much lower performance than all three of these other systems. To achieve the same performance using MCDI as a double-stacked BDI containing three IEMs, for example, four MCDI systems would be needed, which would require a total of eight IEMs (four CEMs and four AEMs). ED with the same number of IEMs as a double-stacked BDI would only utilize two channels each for desalination and concentration because the other two electrode channels use rinsewater or redox active compounds, and thus, ED would

require two additional IEMs to achieve the same performance as a double-stacked BDI. To demonstrate this comparison with ED, the energy consumption of a minimal ED cell, analogous to a double-stacked BDI, was examined by flowing a representative redox couple (10 mM $\text{K}_3[\text{Fe}(\text{CN})_6]$ and 10 mM $\text{K}_4[\text{Fe}(\text{CN})_6]$ in 50 mM NaCl) to two end channels (Figure S10). Under the same experimental conditions (50 mM influent; 0.5 mL/min; 5.7 A/m²), the energy used by an ED cell (0.020 kWh/m³) was comparable to that of the double-stacked BDI (0.016 kWh/m³). However, the decrease in concentration of the desalinated solution in ED was only half of that achieved using BDI. In addition, less energy was consumed using BDI for producing freshwater (0.02–0.16 kWh/m³, influent: 1.5–2.9 g/L) than reported for ED (0.4–2.5 kWh/m³, influent: 1–2.5 g/L),^{2,51–53} although reducing the concentration in the produced water to a similar range as ED (<0.5 g/L) would increase the energy consumption in the BDI system. While the performance of BDI is better than these other electrochemical systems, additional technological advancements could further improve performance, for example, by improving charge utilization and cycle performance for desalination by using more efficient and stable battery electrodes or by other advances that improve cell design through reduced internal resistances.

■ ASSOCIATED CONTENT

Supporting Information

The Supporting Information is available free of charge on the ACS Publications website at DOI: 10.1021/acs.estlett.7b00392.

Detailed information on construction of the cell, energy analyses, electrochemical characterizations of CuHCF electrode, effluent concentration profiles as functions of current density and number of stack, operation of two cells connected in series, batch-mode operation, cycle performance, and comparison with electrodiagnosis. (PDF)

■ AUTHOR INFORMATION

Corresponding Author

*E-mail: blogan@psu.edu. Phone: +1-814-863-7908. Fax: +1-814-863-7304.

ORCID

Christopher A. Gorski: 0000-0002-5363-2904

Bruce E. Logan: 0000-0001-7478-8070

Notes

The authors declare no competing financial interest.

■ ACKNOWLEDGMENTS

This research was supported by the National Science Foundation (CBET-1603635), the King Abdullah University of Science and Technology (KAUST) (OSR-2017-CPF-2907-02), and seed grant funds from Penn State University.

■ REFERENCES

- (1) Elimelech, M.; Phillip, W. A. The future of seawater desalination: energy, technology, and the environment. *Science* **2011**, *333*, 712–717.
- (2) Al-Karaghoul, A.; Kazmerski, L. L. Energy consumption and water production cost of conventional and renewable-energy-powered desalination processes. *Renewable Sustainable Energy Rev.* **2013**, *24*, 343–356.
- (3) Semiat, R. Energy Issues in Desalination Processes. *Environ. Sci. Technol.* **2008**, *42*, 8193–8201.

- (4) Werber, J. R.; Deshmukh, A.; Elimelech, M. The critical need for increased selectivity, not increased water permeability, for desalination membranes. *Environ. Sci. Technol. Lett.* **2016**, *3*, 112–120.

- (5) Zhao, R.; Porada, S.; Biesheuvel, P.; Van der Wal, A. Energy consumption in membrane capacitive deionization for different water recoveries and flow rates, and comparison with reverse osmosis. *Desalination* **2013**, *330*, 35–41.

- (6) Ghaffour, N.; Missimer, T. M.; Amy, G. L. Technical review and evaluation of the economics of seawater desalination: Current and future challenges for better water supply sustainability. *Desalination* **2013**, *309*, 197–207.

- (7) Bar-Zeev, E.; Elimelech, M. Reverse osmosis biofilm dispersal by osmotic back-flushing: cleaning via substratum perforation. *Environ. Sci. Technol. Lett.* **2014**, *1*, 162–166.

- (8) Matin, A.; Khan, Z.; Zaidi, S. M. J.; Boyce, M. C. Biofouling in reverse osmosis membranes for seawater desalination: phenomena and prevention. *Desalination* **2011**, *281*, 1–16.

- (9) Strathmann, H. Electrodialysis, a mature technology with a multitude of new applications. *Desalination* **2010**, *264*, 268–288.

- (10) Suss, M.; Porada, S.; Sun, X.; Biesheuvel, P.; Yoon, J.; Presser, V. Water desalination via capacitive deionization: what is it and what can we expect from it? *Energy Environ. Sci.* **2015**, *8*, 2296–2319.

- (11) Schlumpberger, S.; Lu, N. B.; Suss, M. E.; Bazant, M. Z. Scalable and continuous water deionization by shock electrodialysis. *Environ. Sci. Technol. Lett.* **2015**, *2*, 367–372.

- (12) Kim, S. J.; Ko, S. H.; Kang, K. H.; Han, J. Direct seawater desalination by ion concentration polarization. *Nat. Nanotechnol.* **2010**, *5*, 297–301.

- (13) Ahualli, S.; Iglesias, G. R.; Fernández, M. M.; Jiménez, M. L.; Delgado, Á. V. Use of soft electrodes in capacitive deionization of solutions. *Environ. Sci. Technol.* **2017**, *51*, 5326–5333.

- (14) Zhao, R.; Biesheuvel, P.; Van der Wal, A. Energy consumption and constant current operation in membrane capacitive deionization. *Energy Environ. Sci.* **2012**, *5*, 9520–9527.

- (15) Kim, Y.-J.; Choi, J.-H. Improvement of desalination efficiency in capacitive deionization using a carbon electrode coated with an ion-exchange polymer. *Water Res.* **2010**, *44*, 990–996.

- (16) Kang, J.; Kim, T.; Shin, H.; Lee, J.; Ha, J.-I.; Yoon, J. Direct energy recovery system for membrane capacitive deionization. *Desalination* **2016**, *398*, 144–150.

- (17) Długolecki, P.; van der Wal, A. Energy recovery in membrane capacitive deionization. *Environ. Sci. Technol.* **2013**, *47*, 4904–4910.

- (18) Hatzell, K. B.; Hatzell, M. C.; Cook, K. M.; Boota, M.; Housel, G. M.; McBride, A.; Kumbur, E. C.; Gogotsi, Y. Effect of oxidation of carbon material on suspension electrodes for flow electrode capacitive deionization. *Environ. Sci. Technol.* **2015**, *49*, 3040–3047.

- (19) Jeon, S.-i.; Park, H.-r.; Yeo, J.-g.; Yang, S.; Cho, C. H.; Han, M. H.; Kim, D. K. Desalination via a new membrane capacitive deionization process utilizing flow-electrodes. *Energy Environ. Sci.* **2013**, *6*, 1471–1475.

- (20) Yang, S.; Choi, J.; Yeo, J.-g.; Jeon, S.-i.; Park, H.-r.; Kim, D. K. Flow-electrode capacitive deionization using an aqueous electrolyte with a high salt concentration. *Environ. Sci. Technol.* **2016**, *50*, 5892–5899.

- (21) Cho, Y.; Lee, K. S.; Yang, S.; Choi, J.; Park, H.-r.; Kim, D. K. A novel three-dimensional desalination system utilizing honeycomb-shaped lattice structures for flow-electrode capacitive deionization. *Energy Environ. Sci.* **2017**, *10*, 1746–1750.

- (22) Nativ, P.; Badash, Y.; Gendel, Y. New insights into the mechanism of flow-electrode capacitive deionization. *Electrochem. Commun.* **2017**, *76*, 24–28.

- (23) Ma, J.; He, D.; Tang, W.; Kovalsky, P.; He, C.; Zhang, C.; Waite, T. D. Development of redox-active flow electrodes for high-performance capacitive deionization. *Environ. Sci. Technol.* **2016**, *50*, 13495–13501.

- (24) Choi, J.-H. Determination of the electrode potential causing Faradaic reactions in membrane capacitive deionization. *Desalination* **2014**, *347*, 224–229.

- (25) Kim, T.; Yu, J.; Kim, C.; Yoon, J. Hydrogen peroxide generation in flow-mode capacitive deionization. *J. Electroanal. Chem.* **2016**, *776*, 101–104.
- (26) He, D.; Wong, C. E.; Tang, W.; Kovalsky, P.; Waite, T. D. Faradaic reactions in water desalination by batch-mode capacitive deionization. *Environ. Sci. Technol. Lett.* **2016**, *3*, 222–226.
- (27) Shapira, B.; Avraham, E.; Aurbach, D. Side reactions in capacitive deionization (CDI) processes: the role of oxygen reduction. *Electrochim. Acta* **2016**, *220*, 285–295.
- (28) Tang, W.; He, D.; Zhang, C.; Kovalsky, P.; Waite, T. D. Comparison of Faradaic reactions in capacitive deionization (CDI) and membrane capacitive deionization (MCDI) water treatment processes. *Water Res.* **2017**, *120*, 229–237.
- (29) Dykstra, J. E.; Keesman, K. J.; Biesheuvel, P. M.; van der Wal, A. Theory of pH changes in water desalination by capacitive deionization. *Water Res.* **2017**, *119*, 178–186.
- (30) Srimuk, P.; Ries, L.; Zeiger, M.; Fleischmann, S.; Jäckel, N.; Tolosa, A.; Krüner, B.; Aslan, M.; Presser, V. High performance stability of titania decorated carbon for desalination with capacitive deionization in oxygenated water. *RSC Adv.* **2016**, *6*, 106081–106089.
- (31) Bouhadana, Y.; Avraham, E.; Noked, M.; Ben-Tzion, M.; Soffer, A.; Aurbach, D. Capacitive deionization of NaCl solutions at non-steady-state conditions: inversion functionality of the carbon electrodes. *J. Phys. Chem. C* **2011**, *115*, 16567–16573.
- (32) Pasta, M.; Wessells, C. D.; Cui, Y.; La Mantia, F. A desalination battery. *Nano Lett.* **2012**, *12*, 839–843.
- (33) Lee, J.; Kim, S.; Kim, C.; Yoon, J. Hybrid capacitive deionization to enhance the desalination performance of capacitive techniques. *Energy Environ. Sci.* **2014**, *7*, 3683–3689.
- (34) Kim, S.; Lee, J.; Kim, C.; Yoon, J. Na₂FeP₂O₇ as a novel material for hybrid capacitive deionization. *Electrochim. Acta* **2016**, *203*, 265–271.
- (35) Chen, F.; Huang, Y.; Guo, L.; Ding, M.; Yang, H. Y. A dual-ion electrochemistry deionization system based on AgCl-NMO Electrodes. *Nanoscale* **2017**, *9*, 10101–10108.
- (36) Liu, Y.-H.; Hsi, H.-C.; Li, K.-C.; Hou, C.-H. Electrodeposited manganese dioxide/activated carbon composite as a high-performance electrode material for capacitive deionization. *ACS Sustainable Chem. Eng.* **2016**, *4*, 4762–4770.
- (37) Lee, J.; Kim, S.; Yoon, J. Rocking chair desalination battery based on Prussian Blue electrodes. *ACS Omega* **2017**, *2*, 1653–1659.
- (38) Smith, K. C.; Dmello, R. Na-Ion desalination (NID) enabled by Na-blocking membranes and symmetric Na-intercalation: porous-electrode modeling. *J. Electrochem. Soc.* **2016**, *163*, A530–A539.
- (39) Kim, T.; Logan, B. E.; Gorski, C. A. High power densities created from salinity differences by combining electrode and Donnan potentials in a concentration flow cell. *Energy Environ. Sci.* **2017**, *10*, 1003–1012.
- (40) Smith, K. C. Theoretical evaluation of electrochemical cell architectures using cation intercalation electrodes for desalination. *Electrochim. Acta* **2017**, *230*, 333–341.
- (41) Marino, M.; Kozynchenko, O.; Tennison, S.; Brogioli, D. Capacitive mixing with electrodes of the same kind for energy production from salinity differences. *J. Phys.: Condens. Matter* **2016**, *28*, 114004.
- (42) Kim, T.; Rahimi, M.; Logan, B. E.; Gorski, C. A. Harvesting energy from salinity differences using battery electrodes in a concentration flow cell. *Environ. Sci. Technol.* **2016**, *50*, 9791–9797.
- (43) Chen, F.; Huang, Y.; Guo, L.; Sun, L.; Wang, Y.; Yang, H. Y. Dual-ions electrochemical deionization: a desalination generator. *Energy Environ. Sci.* **2017**, DOI: 10.1039/C7EE00855D.
- (44) Porada, S.; Zhao, R.; Van Der Wal, A.; Presser, V.; Biesheuvel, P. Review on the science and technology of water desalination by capacitive deionization. *Prog. Mater. Sci.* **2013**, *58*, 1388–1442.
- (45) Kim, T.; Yoon, J. CDI ragone plot as a functional tool to evaluate desalination performance in capacitive deionization. *RSC Adv.* **2015**, *5*, 1456–1461.
- (46) Wessells, C. D.; Huggins, R. A.; Cui, Y. Copper hexacyanoferrate battery electrodes with long cycle life and high power. *Nat. Commun.* **2011**, *2*, 550.
- (47) Wang, R. Y.; Wessells, C. D.; Huggins, R. A.; Cui, Y. Highly reversible open framework nanoscale electrodes for divalent ion batteries. *Nano Lett.* **2013**, *13*, 5748–5752.
- (48) Wessells, C. D.; Peddada, S. V.; McDowell, M. T.; Huggins, R. A.; Cui, Y. The effect of insertion species on nanostructured open framework hexacyanoferrate battery electrodes. *J. Electrochem. Soc.* **2012**, *159*, A98–A103.
- (49) Dzombak, D. A.; Ghosh, R. S.; Wong-Chong, G. M. *Cyanide in Water and Soil: Chemistry, Risk, and Management*; CRC Press, 2005.
- (50) Lin, K.; Chen, Q.; Gerhardt, M. R.; Tong, L.; Kim, S. B.; Eisenach, L.; Valle, A. W.; Hardee, D.; Gordon, R. G.; Aziz, M. J.; Marshak, M. P. Alkaline quinone flow battery. *Science* **2015**, *349*, 1529–1532.
- (51) Ortiz, J.; Sotoca, J.; Exposito, E.; Gallud, F.; Garcia-Garcia, V.; Montiel, V.; Aldaz, A. Brackish water desalination by electrodialysis: batch recirculation operation modeling. *J. Membr. Sci.* **2005**, *252*, 65–75.
- (52) Goodman, N. B.; Taylor, R. J.; Xie, Z.; Gozukara, Y.; Clements, A. A feasibility study of municipal wastewater desalination using electrodialysis reversal to provide recycled water for horticultural irrigation. *Desalination* **2013**, *317*, 77–83.
- (53) Ortiz, J.; Exposito, E.; Gallud, F.; García-García, V.; Montiel, V.; Aldaz, A. Desalination of underground brackish waters using an electrodialysis system powered directly by photovoltaic energy. *Sol. Energy Mater. Sol. Cells* **2008**, *92*, 1677–1688.